

Floatable Artificial Leaf to Couple Oxygen-Tolerant CO₂ Conversion with Water Purification

Corresponding Author: Professor Hua Sheng

This file contains all reviewer reports in order by version, followed by all author rebuttals in order by version.

Version 0:

Reviewer comments:

Reviewer #1

(Remarks to the Author)

In this work, Zhang et al. report the design of an artificial leaf that incorporates an In-MOF/GO heterostructure into a porous membrane. This floatable structure enables efficient reduction of dilute CO₂ even in the presence of ambient O₂ levels. Moreover, they demonstrate that this structure is dual-functional, facilitating simultaneous water purification. The concept of a "floatable artificial leaf" is intriguing and holds practical significance in real-environment applications. Additionally, the oxygen tolerance of CO₂ reduction presents considerable challenges, yet is crucial for practical use. The authors achieve a high CO₂ reduction rate in the presence of 20% O₂, which surpasses the performance of most systems operating without O₂.

Given these considerations, I recommend a revision of this manuscript, contingent upon addressing the following issues:

1. For a hybrid photocatalyst, it is essential to clarify the direction of electron transfer within the system. While the authors utilize XPS and theoretical calculations for this purpose, I suggest they include a band structure diagram for further elucidation.
2. The authors claim that the hybrid photocatalyst can generate H₂O₂ from water oxidation in pure water. Selective oxidation of water to H₂O₂ is typically challenging, as it tends to proceed further to O₂. Could the authors explain how this catalyst achieves such selectivity?
3. How does the catalytic performance of In-MOF/GO compare when it is not deposited on the PTFE membrane but instead dispersed individually in water for the catalytic reaction?
4. In the in-situ IR studies shown in Figure 4a, the authors employed D₂O instead of H₂O to observe bands around 1600 cm⁻¹. However, the properties of D₂O differ from those of H₂O, as the mass of D is twice that of H, and the bonding with D is stronger. Could these differences affect the mechanism studies?
5. In the IR studies of CO adsorption, the frequency of adsorbed CO they assigned is very close to that of the free gaseous CO, why did the authors believe this belongs to the adsorbed CO?

Reviewer #2

(Remarks to the Author)

In this manuscript, Zhang et al. report an in-situ growth strategy for fabricating a two-dimensional heterojunction between indium porphyrin metal-organic framework (In-MOF) and graphene oxide (GO). They integrate the In-MOF/GO composite with a porous polytetrafluoroethylene (PTFE) membrane to construct a floating artificial leaf. This artificial leaf can selectively convert CO₂ to CO in a simulated flue gas environment while simultaneously removing pollutants from real water bodies. This study provides a scalable approach for constructing photocatalytic devices for CO₂ conversion in open environments, which is of significant importance. The manuscript is also well-organized and comprehensively introduces this photocatalytic device. The in-situ growth process of In-MOF/GO is clearly demonstrated using characterization methods such as TEM and XRD. The catalytic reaction mechanism is elucidated through in-situ infrared spectroscopy and theoretical calculations. Therefore, I recommend that the manuscript can be considered for acceptance after addressing the following concerns.

Specific revision suggestions are as follows:

1. When using a kinetically controlled growth approach, would changes in the injection rate (either faster or slower) affect the formation of In-MOF/GO?
2. In Figure 2f, it is mentioned that no H₂ is generated. What are the reasons for the suppression of H₂ production?
3. Figures 3a and 3b show that In-MOF/GO has a higher amount of electrons available for catalytic reactions compared to In-

MOF. It is recommended to supplement this with experimental evidence to demonstrate that In-MOF/GO has a higher electron-hole separation efficiency than In-MOF, such as photocurrent measurements and electrochemical impedance spectroscopy (EIS) tests.

4. Why is H₂O₂ generated in the oxidative half-reaction? How is hydrogen peroxide detected? It is recommended to include the detection method and specific steps for measuring hydrogen peroxide in the experimental details section. Also, for the water purification part, what are the major reactive species generated on In-MOF/GO to degrade the pollutants?

5. Suggest citing some relevant literature: Nat. Synth. 2024, DOI: 10.1038/s44160-024-00603-8; 10.1002/anie.202412553

Reviewer #3

(Remarks to the Author)

In this manuscript, the authors reported a 2D heterojunction of In-MOF and GO, which enables the photoreduction of dilute CO₂ even in the presence of O₂. Furthermore, the photocatalyst could be further integrated with PTFE membrane to create a floatable artificial leaf for CO₂ photoreduction coupled with contaminant removal. This study presents an intriguing case of aerobic CO₂ reduction. However, some major concerns should be addressed before it is considered for publication.

1. Given the authors' emphasis on the floatable configuration, what are the unique advantages of the triphase system? In addition, how does the catalytic performance compare in the traditional solid-liquid biphasic system?

2. The photoelectronic properties of the photocatalysts, including UV/Vis spectra and band positions, are entirely overlooked. These properties are crucial for demonstrating the thermodynamic feasibility of simultaneous CO₂ reduction and 2e⁻/4e⁻ water oxidation.

3. What role does GO play during the photocatalytic reactions in this study?

4. It is recommended to provide more experimental details of photocatalytic tests, including the light intensity, the thickness and light transmittance of the PTFE film.

5. To comprehensively investigate the chemisorption properties and interfacial interactions of the photocatalyst with carbon dioxide and oxygen, it is imperative to perform temperature-programmed desorption (TPD) experiments using pure CO₂, O₂, and a CO₂/O₂ mixture. This analytical technique will provide valuable insights into the adsorption capacity and the strength of the bonding between the catalyst surface and the adsorbate molecules.

6. As mentioned in this manuscript: "electron densities on the GO and In-MOF moieties decrease and increase, respectively, indicating electron transfer from GO to In-MOF during the formation of the heterostructure". What is causing this phenomenon, and what is the underlying driving force?

Version 1:

Reviewer comments:

Reviewer #1

(Remarks to the Author)

Now I think this paper should be published at present form.

Reviewer #2

(Remarks to the Author)

The author has addressed the reviewer's concerns, and I suggest publishing this work.

Reviewer #3

(Remarks to the Author)

The authors have well addressed the issues I had on its original version. Thus, I support the acceptance of this manuscript.

Open Access This Peer Review File is licensed under a Creative Commons Attribution 4.0 International License, which permits use, sharing, adaptation, distribution and reproduction in any medium or format, as long as you give appropriate credit to the original author(s) and the source, provide a link to the Creative Commons license, and indicate if changes were made.

In cases where reviewers are anonymous, credit should be given to 'Anonymous Referee' and the source.

The images or other third party material in this Peer Review File are included in the article's Creative Commons license, unless indicated otherwise in a credit line to the material. If material is not included in the article's Creative Commons license and your intended use is not permitted by statutory regulation or exceeds the permitted use, you will need to obtain permission directly from the copyright holder.

To view a copy of this license, visit <https://creativecommons.org/licenses/by/4.0/>

Responds to the reviewers' comments:

Reviewer #1:

Comment:

In this work, Zhang et al. report the design of an artificial leaf that incorporates an In-MOF/GO heterostructure into a porous membrane. This floatable structure enables efficient reduction of dilute CO₂ even in the presence of ambient O₂ levels. Moreover, they demonstrate that this structure is dual-functional, facilitating simultaneous water purification. The concept of a "floatable artificial leaf" is intriguing and holds practical significance in real-environment applications. Additionally, the oxygen tolerance of CO₂ reduction presents considerable challenges, yet is crucial for practical use. The authors achieve a high CO₂ reduction rate in the presence of 20% O₂, which surpasses the performance of most systems operating without O₂. Given these considerations, I recommend a revision of this manuscript, contingent upon addressing the following issues:

Response:

We thank the reviewer for this positive comment. In the following, we have provided detailed responses to the comments and revised the manuscript accordingly. We hope that the revised version meets the Reviewer #1's expectations and is now suitable for publication in *Nature Communications*.

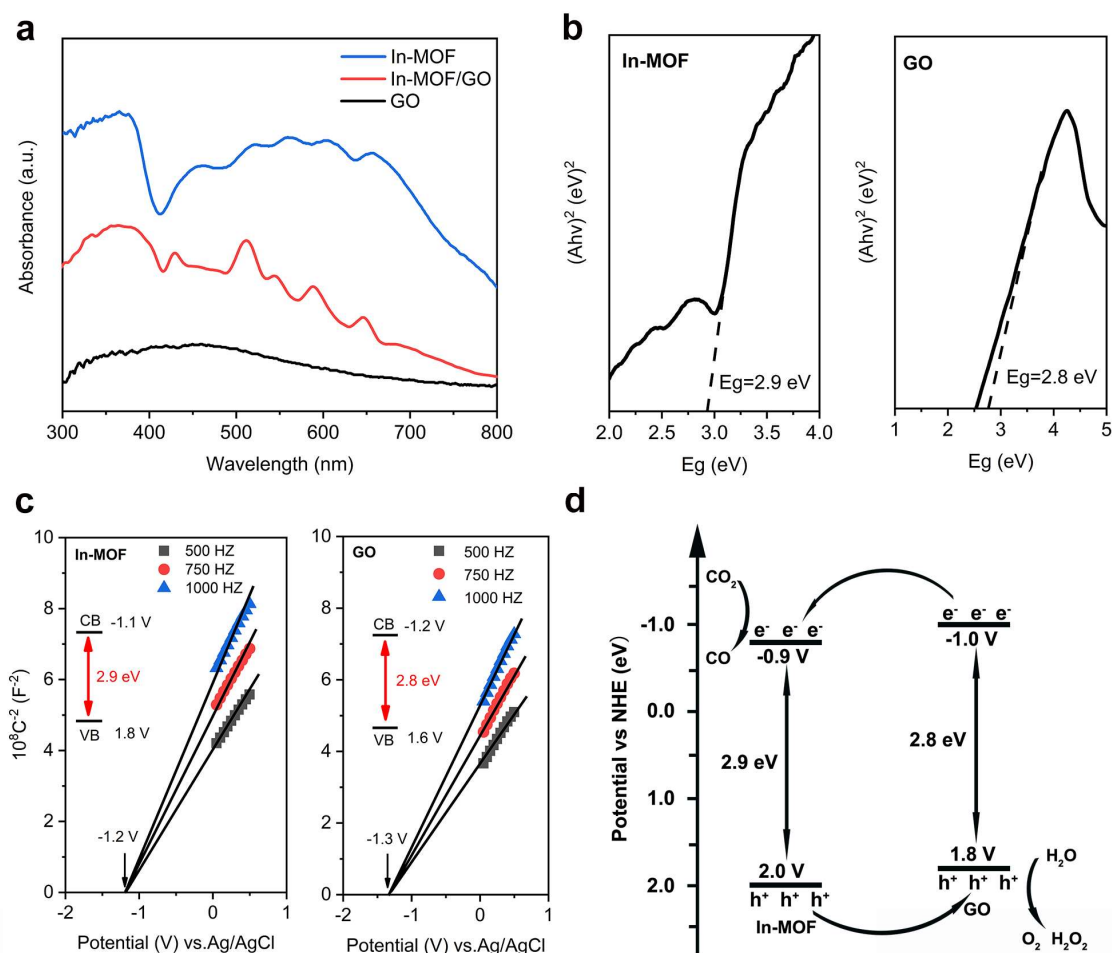
1. Comment:

For a hybrid photocatalyst, it is essential to clarify the direction of electron transfer within the system. While the authors utilize XPS and theoretical calculations for this purpose, I suggest they include a band structure diagram for further elucidation.

Response:

We thank the reviewer for the valuable comments. Based on this comment, we have performed additional tests, as illustrated in the figure below. UV-vis spectra were used to generate Tauc plots to determine the bandgap energies (**Supplementary Fig. 16a**). From the Tauc plots (**Supplementary Fig. 16b**), we determined that the bandgaps of In-MOF and GO are 2.9 eV and 2.8 eV, respectively. The Mott-Schottky plots (**Supplementary Fig. 16c**) show positive slopes

for both In-MOF and GO, indicating that both materials are n-type semiconductors. The flat-band potentials of In-MOF and GO were found to be -1.2 V and -1.3 V vs. Ag/AgCl, respectively. Considering that the conduction band potentials of n-type semiconductors are typically 0.1 V more negative than the flat-band potentials, the conduction band potentials of In-MOF and GO are therefore -1.1 V and -1.2 V vs. Ag/AgCl, respectively. Taking the band gap into account, the conduction band potentials of In-MOF and GO are therefore -1.1 V and -1.2 V vs. Ag/AgCl, respectively. Taking the band gap into account, the band structure of In-MOF was determined as -0.9 V and 2.0 V vs. NHE for conduction and valence band potentials, respectively, while GO's conduction band and valence band potentials were found to be -1.0 V and 1.8 V vs. NHE, as shown in **Supplementary Fig. 16d**. Based on these band levels of In-MOF and GO, also considering the XPS and theoretical results, In-MOF and GO form a type-II heterojunction, in which the conduction band potential of In-MOF is more negative than the required potential for CO₂ reduction to CO (-0.53 V), while the valence band potential of GO more positive than the potentials required for the oxidation of H₂O to H₂O₂ (+1.78 V) and O₂ (+1.23 V). Therefore, the In-MOF/GO heterojunction is theoretically capable of simultaneously facilitating both CO₂ reduction and water oxidation.



Supplementary Fig. 16. (a) UV-vis spectra of In-MOF, GO and In-MOF/GO-4h; (b) Tauc plots of In-MOF and GO; (c) Mott–Schottky plots of In-MOF and GO; (d) Schematic illustration of the band structure of In-MOF/GO heterojunction.

Changes in Manuscript:

We have added the following discussion to the "**Investigation of preferential CO₂ adsorption**" section:

“The bandgaps of In-MOF and GO were determined using Tauc plots derived from UV-vis spectroscopy, while the conduction band potentials were established through Mott-Schottky analysis, allowing for the construction of the band structure diagram. In-MOF exhibits a less negative conduction band level (-0.9 V vs. NHE) compared to GO (-1.0 V), but a more positive valence band level (2.0 V vs. NHE) than GO (1.8 V). As a result, they are likely to form a type-II heterojunction, with the electron transfer occurring from GO to In-MOF and hole transfer from In-MOF to GO (Supplementary Fig. 16).”

Changes in Supporting Information:

Supplementary Fig. 16 has been added, along with the discussion:

“UV-vis spectra were converted into Tauc plots to determine the bandgap energy (Supplementary Fig. 16a). From these Tauc plots (Supplementary Fig. 16b), we determined that the bandgaps of In-MOF and GO are 2.9 eV and 2.8 eV, respectively. In the Mott-Schottky plots (Supplementary Fig. 16c), In-MOF and GO both exhibit positive slopes, indicating that both are n-type semiconductors. The flat-band potentials of In-MOF and GO were found to be -1.2 V and -1.3 V vs. Ag/AgCl, respectively. Considering that the conduction band potentials of n-type semiconductors are typically 0.1 V more negative than their flat-band potentials, the conduction band potentials of In-MOF and GO were determined to be -1.1 V and -1.2 V vs. Ag/AgCl, respectively. Based on the 2.9 eV bandgap of In-MOF, its valence band potential was calculated to be 1.8 V vs. Ag/AgCl; while for GO with a bandgap of 2.8 eV, the valence band potential was determined to be 1.6 V vs. Ag/AgCl. After converting between Ag/AgCl and NHE, the conduction and valence band potential of In-MOF is -0.9 V and 2.0 V vs. NHE, respective; for GO, its conduction and valence band potential is -1.0 V and 1.8 V vs. NHE, respectively. Therefore, we illustrated the band structure diagram as Supplementary Fig. 16d, which clearly shows that In-MOF and GO are likely to form a type-II heterojunction.”

2. Comment:

The authors claim that the hybrid photocatalyst can generate H₂O₂ from water oxidation in pure water. Selective oxidation of water to H₂O₂ is typically challenging, as it tends to proceed further to O₂. Could the authors explain how this catalyst achieves such selectivity?

Response:

We sincerely thank the reviewer for raising this important question. We believe that the net yield of H₂O₂ in a photocatalytic system by the balance between its generation and decomposition. The H₂O₂ produced during water oxidation can either be reduced back to water via electrons ($\text{H}_2\text{O}_2 + 2\text{e}^- + 2\text{H}^+ \rightarrow 2\text{H}_2\text{O}$) or oxidized to oxygen via holes ($\text{H}_2\text{O}_2 + 2\text{H}^+ \rightarrow \text{O}_2 + 2\text{H}_2\text{O}$). Thus, the low concentration of H₂O₂ detected in a photocatalytic system is often owing to its rapid decomposition. In comparison to the typical liquid-solid systems, the use of a tri-phase system significantly reduces the decomposition rate of H₂O₂, as demonstrated and discussed in our recent work (*Energy Environ. Sci.* **2024**, *17*, 4725). Two main factors contribute to this decelerated decomposition: firstly, hydrogen peroxide formed under triphasic conditions can diffuse more effectively into the bulk aqueous solution, reducing the chances of recontacting the catalyst and undergoing further reactions; secondly, in a triphasic system, some active sites of the photocatalyst are exposed to the gas phase, thereby reducing the direct interaction with hydrogen peroxide in the aqueous solution, which further decreases the likelihood of decomposition. Based on these factors, a triphasic catalytic system is more conducive to the selective production of high-value hydrogen peroxide, as also supported by Zhang's recent work (*Angew. Chem. Int. Ed.* **2022**, *134*, e202200802).

3. Comment:

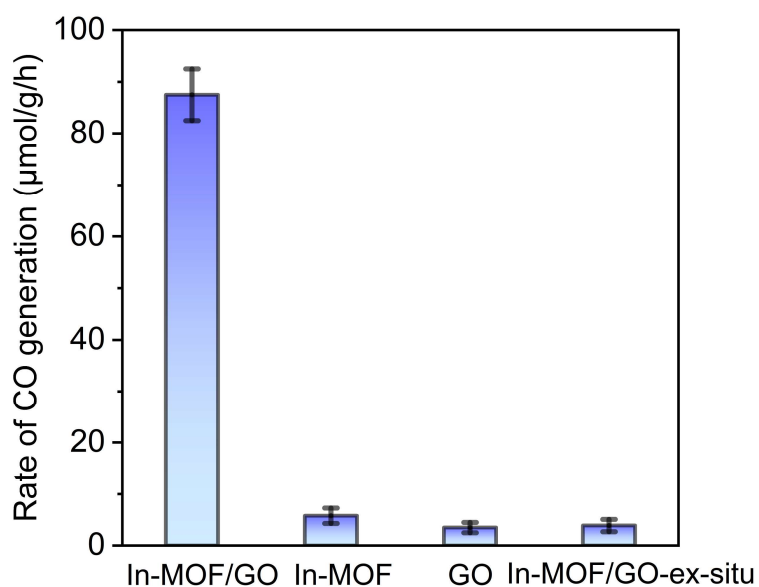
How does the catalytic performance of In-MOF/GO compare when it is not deposited on the PTFE membrane but instead dispersed individually in water for the catalytic reaction?

Response:

We sincerely thank the reviewer for raising this important question. Based on this comment, we have conducted additional performance tests by directly dispersing the catalyst powders in water. In this work, the triphasic setup enabled a CO generation rate of 762.5 $\mu\text{mol} \cdot \text{g}^{-1} \cdot \text{h}^{-1}$ on In-MOF/GO. However, when the same catalyst powders were directly dispersed in water in a traditional solid-water system, as shown in **Supplementary Fig. 6** below, the CO generation rate

on In-MOF/GO significantly declined to $87.5 \mu\text{mol} \cdot \text{g}^{-1} \cdot \text{h}^{-1}$.

The main factor limiting the rate of CO_2 reduction in this typical water-solid reaction is the low concentration and diffusion rate of CO_2 in water. In contrast, when the catalysts are integrated into a floatable PTFE membrane, the CO_2 reduction occurs in a triphasic system. The hydrophobic PTFE pore structure acts as a diffusion layer, facilitating the transportation of gaseous CO_2 to the catalyst surface, which significantly enhances the local concentration of CO_2 and accelerates the CO_2 reduction rate. This explains the reason why we try to fabricate a “floatable artificial leaf” in this work.



Supplementary Fig. 6. Comparison of CO generation rates from aerobic CO_2 reduction on In-MOF/GO, In-MOF, GO, and In-MOF/GO-ex-situ, when directly dispersing these catalyst powders in water instead of integrating into floatable PTFE membrane.

Changes in Manuscript:

We have added the following discussion to the "Photocatalytic activity test" section:

“Notably, when MOF/GO-4h powders were directly dispersed in water and tested for photocatalytic activity without being integrated into a floatable device, a significant decrease in the CO generation rate ($87.5 \mu\text{mol} \cdot \text{g}^{-1} \cdot \text{h}^{-1}$) was observed (Supplementary Fig. 6), highlighting the clear advantage of employing a floatable system.”

Changes in Supporting Information:

Supplementary Fig. 6 has been added to the Supporting Information.

4. Comment:

In the in-situ IR studies shown in Figure 4a, the authors employed D₂O instead of H₂O to observe bands around 1600 cm⁻¹. However, the properties of D₂O differ from those of H₂O, as the mass of D is twice that of H, and the bonding with D is stronger. Could these differences affect the mechanism studies?

Response:

We are very grateful to the reviewer for raising this question. We believe that the use of D₂O will not affect the study of the mechanism, and in fact, substituting D₂O for H₂O offers several advantages. Firstly, our goal is to monitor the structural changes of the carboxylate-coordinated In-node during the photocatalytic reactions. However, the IR bands for carboxylate overlap with the bending vibration of H₂O (~1630 cm⁻¹). Substituting H₂O with D₂O (~1210 cm⁻¹) opens up the IR window in this region, making changes in specific functional groups or intermediates in this region more evident, thereby improving the quality of data interpretation. Secondly, as noted by the reviewer, the larger mass of D compared to H makes the O-D bond stronger than O-H bond. This results in a slower water oxidation reaction when using D₂O. Also for CO₂ reduction, which relies on protons released from water oxidation ($\text{H}_2\text{O} + 4\text{h}^+ \rightarrow \text{O}_2 + 4\text{H}^+$) to facilitate the formation of *COOH, the use of D₂O similarly slows down the reaction rate. In in-situ spectroscopic studies, a slower reaction rate is advantageous, as it facilitates the capture and observation of intermediate species. In fact, we also conducted IR studies with H₂O, and the results showed that the IR bands of *COOH intermediates appeared at the same wavenumbers for both H₂O and D₂O. However, the bands observed with D₂O were more intensified, likely due to the relatively slower kinetics.

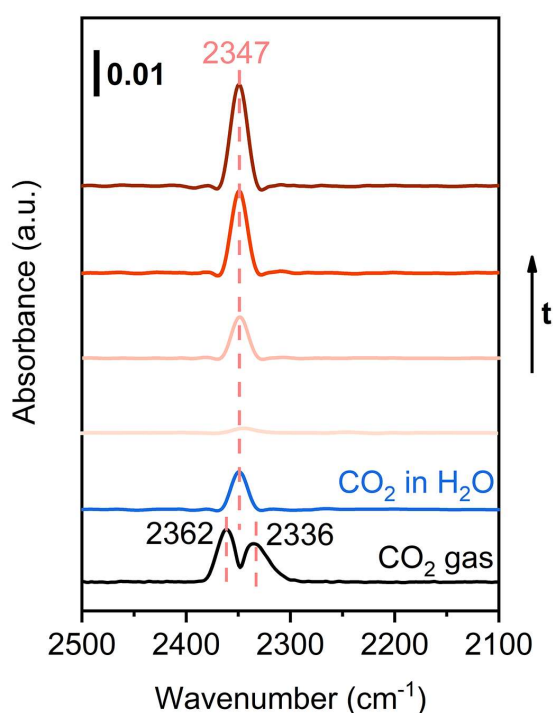
5. Comment:

In the IR studies of CO₂ adsorption, the frequency of adsorbed CO₂ they assigned is very close to that of the free gaseous CO₂, why did the authors believe this belongs to the adsorbed CO₂?

Response:

We sincerely thank the reviewer for raising this question. The explanation is provided below the **Supplementary Fig. 20**, and we kindly refer to the figure below. As shown in this figure, the

standard gaseous CO_2 exhibits a doublet band at 2362 and 2336 cm^{-1} , corresponding to the P and R branches, which arise from rotation transition of the CO_2 molecule. In contrast, when CO_2 is dissolved in water, as characterized by IR in attenuated total reflection (ATR) mode, it exhibits a singlet band around 2347 cm^{-1} . This shift originates from the interaction between CO_2 and solvent water via hydrogen bonding, which restricts the rotating vibration of CO_2 molecules and thus eliminates the band splitting. In the case of In-MOF/GO, we observed the CO_2 band at around 2347 cm^{-1} , which is identical to that of dissolved CO_2 . Based on this observation, we conclude that the adsorption of CO_2 on In-MOF/GO forms a similar hydrogen-bonded structure with surface hydroxyl groups of In-node.



Supplementary Fig. 20. FT-IR spectra sequence collected during the CO_2 adsorption in the dark.

Changes in Supporting Information:

We have added the following discussion below Supplementary Fig. 20:

“The standard gaseous CO_2 exhibits a doublet band at 2362 and 2336 cm^{-1} , corresponding to the P and R branches, which arise from rotation transition of the CO_2 molecule. In contrast, when CO_2 is dissolved in water, as characterized by IR in attenuated total reflection (ATR) mode, it exhibits a singlet band around 2347 cm^{-1} . This shift originates from the interaction between CO_2 and solvent water via hydrogen bonding, which restricts the rotating vibration of CO_2 molecules

and thus eliminates the band splitting. In the case of In-MOF/GO, we observed the CO₂ band at around 2347 cm⁻¹, which is identical to that of dissolved CO₂. Based on this observation, also consider the gradually depletion of the surface hydroxy groups at 3612 cm⁻¹, we conclude that the adsorption of CO₂ on In-MOF/GO forms a similar hydrogen-bonded structure with surface hydroxyl groups of In-node.”

Reviewer #2:**Comment:**

In this manuscript, Zhang et al. report an in-situ growth strategy for fabricating a two-dimensional heterojunction between indium porphyrin metal-organic framework (In-MOF) and graphene oxide (GO). They integrate the In-MOF/GO composite with a porous polytetrafluoroethylene (PTFE) membrane to construct a floating artificial leaf. This artificial leaf can selectively convert CO₂ to CO in a simulated flue gas environment while simultaneously removing pollutants from real water bodies. This study provides a scalable approach for constructing photocatalytic devices for CO₂ conversion in open environments, which is of significant importance. The manuscript is also well-organized and comprehensively introduces this photocatalytic device. The in-situ growth process of In-MOF/GO is clearly demonstrated using characterization methods such as TEM and XRD. The catalytic reaction mechanism is elucidated through in-situ infrared spectroscopy and theoretical calculations. Therefore, I recommend that the manuscript can be considered for acceptance after addressing the following concerns.

Response:

We thank the reviewer for this positive comment. In the following, we have provided detailed responses to the comments and revised the manuscript accordingly. We hope that the revised version meets the Reviewer #2's expectations and is now suitable for publication in *Nature Communications*.

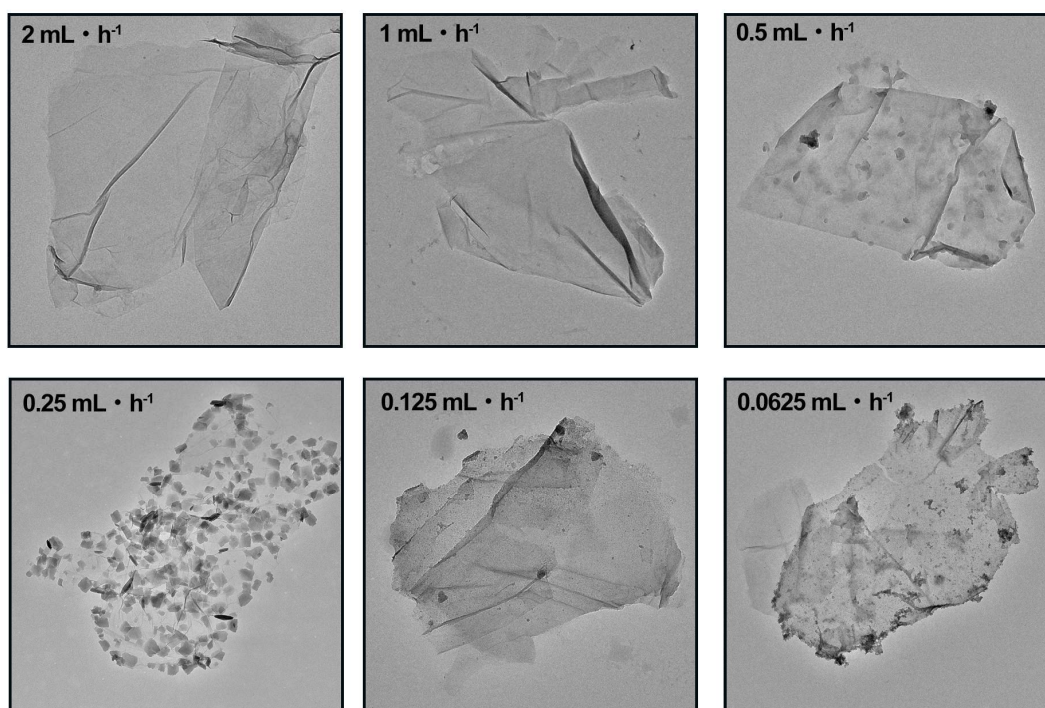
1. Comment:

When using a kinetically controlled growth approach, would changes in the injection rate (either faster or slower) affect the formation of In-MOF/GO?

Response:

We are very grateful to the reviewer for raising this question. Based on this comment, we adjusted the injection rate during the synthesis of In-MOF/GO and obtained samples at six different injection rates. The TEM images of these samples are shown in the figure below. Our findings indicate that the speed of the injection rate affects the formation of In-MOF/GO. At injection rates of 2 and 1 mL·h⁻¹, we observed almost no In-MOF nanosheets on the GO surface. At an injection rate of 0.5 mL·h⁻¹, only a small amount of In-MOF nanosheets formed, possibly due to the rapid

nucleation rate leading to MOF crystals nucleating in the solution rather than on the GO surface. Conversely, when the injection rate was too slow ($0.125 \text{ mL}\cdot\text{h}^{-1}$ and $0.0625 \text{ mL}\cdot\text{h}^{-1}$), a punctate morphology appeared on the GO surface without the formation of In-MOF nanosheets. At these slower rates, the local concentration gradually increased but did not rapidly reach the critical concentration required for forming larger crystals. Consequently, while numerous nucleation sites form, the insufficient material supply inhibited further growth, resulting in the formation of many small MOF particles or clusters instead. Therefore, to achieve well-formed In-MOF/GO structures, it is essential to strictly control the injection rate. Only at an injection rate of $0.25 \text{ mL}\cdot\text{h}^{-1}$ was the ideal In-MOF/GO structure successfully achieved.



Supplementary Fig. 1. TEM images of In-MOF/GO synthesized at different injection rates.

Changes in Manuscript:

We have added the following discussion to the "Characterization of photocatalysts" section:

"Injection rates that are too fast or too slow can affect the formation of In-MOF/GO (Supplementary Fig. 1)."

Changes in Supporting Information:

Supplementary Fig. 1 has been added, along with the discussion:

“When the injection rate was set to 2 and 1 mL·h⁻¹, there were virtually no In-MOF nanosheets observed on GO. At an injection rate of 0.5 mL·h⁻¹, only a small amount of In-MOF nanosheets formed, possibly due to the rapid nucleation rate leading to MOF crystals nucleating in the solution rather than on the GO surface. Conversely, when the injection rate was too slow (0.125 mL·h⁻¹ and 0.0625 mL·h⁻¹), a punctate morphology appeared on the GO surface without the formation of In-MOF nanosheets. At these slow injection rates, the local concentration in the system gradually increases but does not rapidly reach the critical concentration necessary for the formation of larger crystals. Consequently, while numerous nucleation sites may form, insufficient material supply to support their further growth results in the formation of many small MOF particles or clusters instead. Therefore, to achieve well-formed In-MOF/GO structures, it is essential to strictly control the injection rate. Only at an injection rate of 0.25 mL·h⁻¹ was the ideal In-MOF/GO structure successfully achieved.”

2. Comment:

In Figure 2f, it is mentioned that no H₂ is generated. What are the reasons for the suppression of H₂ production?

Response:

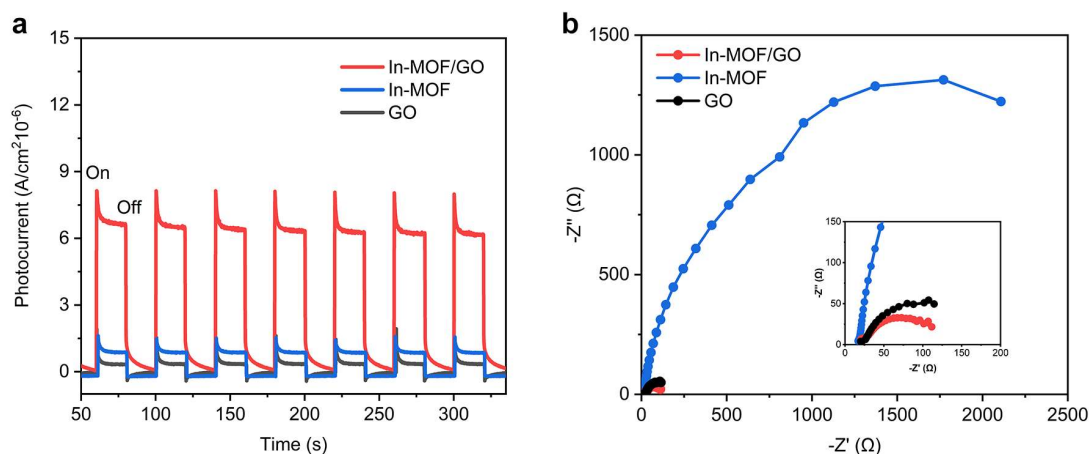
We sincerely thank the reviewer for raising this question. First, the analysis of adsorption-desorption isotherms, IR spectra and TPD results demonstrates a strong affinity of CO₂ for the In-MOF/GO structure, which originates from acid-base interactions between CO₂ and surface hydroxyl groups on the In-node. This affinity facilitates CO₂ occupation on surface sites over water molecules, favoring CO₂ reduction over H₂ production. Additionally, the employment of a triphasic system is essential in this process. In this work, the hydrophobic PTFE membrane pores function as a gas-diffusion layer, with a hydrophobic-hydrophilic abrupt interface that efficiently transports gaseous CO₂ to the surface of the photocatalyst. Compared to the typical water-solid system, which is limited by CO₂'s low solubility and diffusion rate in water, this triphasic setup enhances the local CO₂ concentration, further suppressing the H₂ production. Our recent work (*Energy Environ. Sci.* **2024**, *17*, 4725) and another study by Zhang et al. (*Angew. Chem. Int. Ed.* **2022**, *134*, e202200802) both demonstrate that switching from water-solid to triphasic system significantly promotes CO₂ reduction selectivity over H₂ production for the same photocatalyst.

3. Comment:

Figures 3a and 3b show that In-MOF/GO has a higher amount of electrons available for catalytic reactions compared to In-MOF. It is recommended to supplement this with experimental evidence to demonstrate that In-MOF/GO has a higher electron-hole separation efficiency than In-MOF, such as photocurrent measurements and electrochemical impedance spectroscopy (EIS) tests.

Response:

We thank the reviewer for the valuable suggestion. Based on this comment, we have added photocurrent measurements and electrochemical impedance spectroscopy (EIS) tests. Please refer to the figure below. The results show that In-MOF/GO exhibits the highest phot-current response and the lowest impedance, indicating that In-MOF/GO has the highest electron-hole separation efficiency, which is also the reason for its excellent catalytic performance.



Supplementary Fig. 17. Photocurrent measurements (a) and electrochemical impedance spectroscopy (b) for In-MOF/GO, In-MOF, and GO.

Changes in Manuscript:

We have added the following discussion to the "*Investigation of preferential CO₂ adsorption*" section:

"The formation of the heterojunction was further confirmed by photocurrent and electrochemical impedance spectroscopy (EIS) measurements, which indicate that the hybrid In-MOF/GO exhibits significantly enhanced electron-hole separation capabilities compared to individual In-MOF or GO (Supplementary Fig. 17)."

Changes in Supporting Information:

Supplementary Fig. 17 has been added, along with the discussion:

“In the photocurrent measurements, the photocurrent of In-MOF/GO is 7 and 10 times higher than that of individual In-MOF and GO, respectively. EIS analysis further shows that the hybrid structure exhibits significantly lower impedance, supporting the improved electron-hole separation efficiency in the hybrid catalyst, due to the formation of the type-II heterojunction.”

4. Comment:

Why is H₂O₂ generated in the oxidative half-reaction? How is hydrogen peroxide detected? It is recommended to include the detection method and specific steps for measuring hydrogen peroxide in the experimental details section. Also, for the water purification part, what are the major reactive species generated on In-MOF/GO to degrade the pollutants?

Response:

We are very grateful to the reviewer for raising this question and for the valuable suggestions. While O₂ is the primary product of water oxidation in many photocatalytic systems, this does not preclude H₂O₂ generation during the process. The challenge in obtaining H₂O₂ as a final product lies in its instability: it can undergo further oxidation to O₂ or reduction back to water. Achieving effective net H₂O₂ production requires minimizing its subsequent decomposition, both oxidative and reductive. Compared to a typical water-solid reaction, in a triphasic system where the reaction occurs at the gas-water boundary, H₂O₂, once generated and diffused into the bulk water phase, is far less likely to diffuse back to the catalyst surface. In our recent work (*Energy Environ. Sci.* **2024**, *17*, 4725), we demonstrated the H₂O₂ decomposition rate in a triphasic system is significantly slower than a water-solid setup using the same photocatalyst. Therefore, the observation of H₂O₂ generation in this study is primarily attributed to the triphasic system, which minimizes H₂O₂ decomposition and thereby enhances net H₂O₂ production.

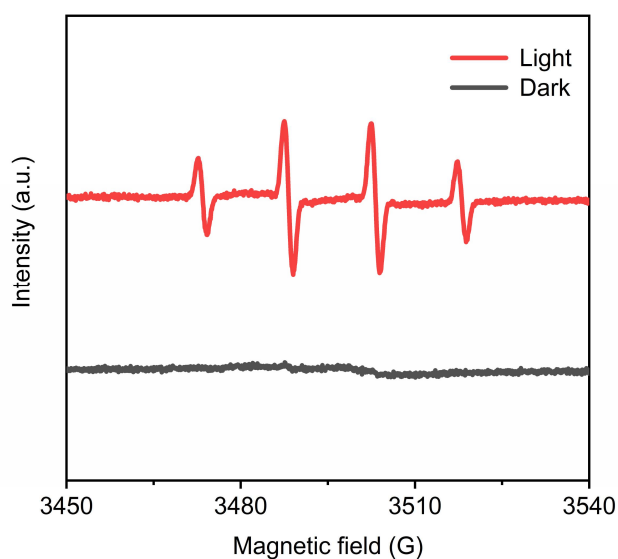
For the detection method, we have added the details to the "**Methods**" section of the manuscript. The specific steps are as follows:

H₂O₂ detection

The hydrogen peroxide (H₂O₂) was quantified by DPD-POD method³⁰. The DPD (N, N-diethyl-p-phenylenediamine) solution was prepared by dissolving 0.1 g of DPD in 10 mL of 0.05 M H₂SO₄. The POD (peroxidase from horseradish) solution was prepared by dissolving 10 mg of POD in 10 mL of deionized water. A phosphate buffer solution was prepared by adding 6 g of potassium

dihydrogen phosphate and 1.68 g of dipotassium phosphate to 100 mL of deionized water. All prepared solutions were stored in a refrigerator. For the measurement of H_2O_2 , 2 mL of the photocatalyzed solution was mixed with 0.4 mL of the phosphate buffer, 3 mL of water, 0.05 mL of DPD, and 0.05 mL of POD, followed by shaking for 45 seconds. The resulting solution was analyzed using UV-vis spectroscopy. When the generated H_2O_2 exceeded the detection limit, a pink-colored solution was obtained, and the H_2O_2 concentration was determined by measuring the absorbance at approximately 552 nm.

For the possible reactive species in water purification, in addition to the photogenerated holes and detected H_2O_2 , both of which possess sufficient oxidative power for the removal of aqueous contaminants, the presence of other reactive radical species, such as $\cdot\text{OH}$, should also be investigated. To this end, we have included *in situ* EPR testing, as shown in the figure below, where $\cdot\text{OH}$ radicals were detected under light irradiation. This $\cdot\text{OH}$ radicals may be produced either through water oxidation or from the reduction of in-situ generated H_2O_2 . Given the high oxidative capacity of $\cdot\text{OH}$ radicals, they also contribute to the degradation of aqueous contaminants.



Supplementary Fig. 14. *In-situ* EPR testing of In-MOF/GO with the use of DMPO (3,4-dihydro-2,3-dimethyl-2H-pyrrole 1-oxide) as spin-trapper.

Changes in Manuscript:

We have added the details of H_2O_2 detection approach to the "**Methods**" section of the manuscript as listed in the **Response**.

We have added the following discussion to the "**Photocatalytic activity test**" section of the manuscript:

"The in situ EPR analysis also confirmed presence of hydroxyl radicals, which may also contribute to the removal of aqueous contaminants (Supplementary Fig. 14)."

Changes in Supporting Information:

Supplementary Fig. 14 was added, along with the discussion:

"In the dark environment, no signals were detected (black trace); however, after 10 minutes of in-situ light irradiation, hydroxyl radicals were detected (red trace). This indicates that hydroxyl radicals were generated during the photocatalytic process, either through water oxidation or from the reduction of in-situ generated H₂O₂. Given the high oxidative capacity of ·OH radicals, they also contribute to the degradation of aqueous contaminants."

5. Comment:

Suggest citing some relevant literature: *Nat. Synth.* 2024, DOI: 10.1038/s44160-024-00603-8; 10.1002/anie.202412553

Response:

We thank the reviewer for the valuable suggestion. The corresponding literatures (*Nat. Synth.* 2024, 3, 1404 and *Angew. Chem. Int. Ed.* 2024, 63, e202412553) have been cited as Ref 9 and 10 in the manuscript.

Reviewer #3:**Comment:**

In this manuscript, the authors reported a 2D heterojunction of In-MOF and GO, which enables the photoreduction of dilute CO₂ even in the presence of O₂. Furthermore, the photocatalyst could be further integrated with PTFE membrane to create a floatable artificial leaf for CO₂ photoreduction coupled with contaminant removal. This study presents an intriguing case of aerobic CO₂ reduction. However, some major concerns should be addressed before it is considered for publication.

Response:

We thank the reviewer for this positive comment. In the following, we have provided detailed responses to the comments and revised the manuscript accordingly. We hope that the revised version meets the Reviewer #3's expectations and is now suitable for publication in *Nature Communications*.

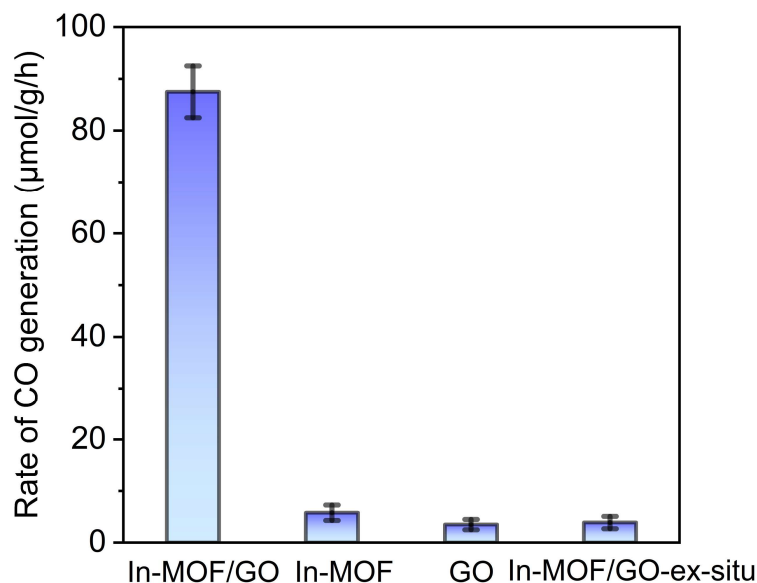
1. Comment:

Given the authors' emphasis on the floatable configuration, what are the unique advantages of the triphase system? In addition, how does the catalytic performance compare in the traditional solid-liquid biphasic system?

Response:

We are very grateful to the reviewer for raising this question. In our opinion, the triphasic system is particularly suitable for photocatalytic reactions involving gaseous reactants. In traditional water-soild biphasic system for CO₂ reduction, the main limiting factor is the low solubility and diffusion rate of CO₂ in water. In contrast, in a triphasic reaction, where reactions occur at the gas-water interface, the transportation of gaseous CO₂ to the catalyst's surface sites is significantly enhanced, especially through the use of the gas diffusion layer upon the catalysts (such as the hydrophobic PTFE pore structure in this study). This setup substantially increases the local concentration of CO₂ near the catalyst surface, thereby accelerating the CO₂ reduction rate. In this work, the triphasic setup enabled a CO generation rate of 762.5 μmol·g⁻¹·h⁻¹ on In-MOF/GO. However, when the catalyst powders were directly dispersed in water in a traditional solid-water system, as shown in **Supplementary Fig. 6** below, the CO generation rate on In-MOF/GO

significantly declined to $87.5 \mu\text{mol} \cdot \text{g}^{-1} \cdot \text{h}^{-1}$. This result highlights the advantages of the triphasic system for enhancing photocatalytic reaction efficiency.



Supplementary Fig. 6. Comparison of CO generation rates from aerobic CO_2 reduction on In-MOF/GO, In-MOF, GO, and In-MOF/GO-ex-situ, when directly dispersing these catalyst powders in water instead of integrating into floatable PTFE membrane.

Another advantage of the tri-phasic reaction is its optimization of product diffusion from the catalyst surface. At the gas-water interface, gaseous products can easily be released into the gas phase, while water-soluble products can diffuse into the bulk liquid, preventing back-reaction or over-reaction. In the case of water oxidation, although O_2 is the primary product in many photocatalytic systems, this does not preclude H_2O_2 generation during the process. The challenge in obtaining H_2O_2 as a final product lies in its instability: it can undergo further oxidation to O_2 or reduction back to water. Achieving effective net H_2O_2 production requires minimizing its subsequent decomposition, both oxidative and reductive. Compared to a typical water-solid reaction, in a triphasic system where the reaction occurs at the gas-water boundary, H_2O_2 , once generated and diffused into the bulk water phase, is far less likely to diffuse back to the catalyst surface to be decomposed. In our recent work (*Energy Environ. Sci.* **2024**, *17*, 4725), we demonstrated the H_2O_2 decomposition rate in a triphasic system is significantly slower than a water-solid setup using the same photocatalyst. In this study, a H_2O_2 generation rate of $212.5 \mu\text{mol} \cdot \text{g}^{-1} \cdot \text{h}^{-1}$ was achieved in the floatable system, while in the dispersed biphasic system, almost

no H₂O₂ generation was detected. Therefore, the triphasic system effectively minimizes H₂O₂ decomposition and thereby enhances net H₂O₂ production.

Changes in Manuscript:

We have added the following discussion to the "Photocatalytic activity test" section:

*“Notably, when MOF/GO-4h powders were directly dispersed in water and tested for photocatalytic activity without being integrated into a floatable device, a significant decrease in the CO generation rate ($87.5 \mu\text{mol} \cdot \text{g}^{-1} \cdot \text{h}^{-1}$) was observed (**Supplementary Fig. 6**), highlighting the clear advantage of employing a floatable system.”*

Changes in Supporting Information:

Supplementary Fig. 6 has been added.

2. Comment:

The photoelectronic properties of the photocatalysts, including UV/vis spectra and band positions, are entirely overlooked. These properties are crucial for demonstrating the thermodynamic feasibility of simultaneous CO₂ reduction and 2e/4e water oxidation.

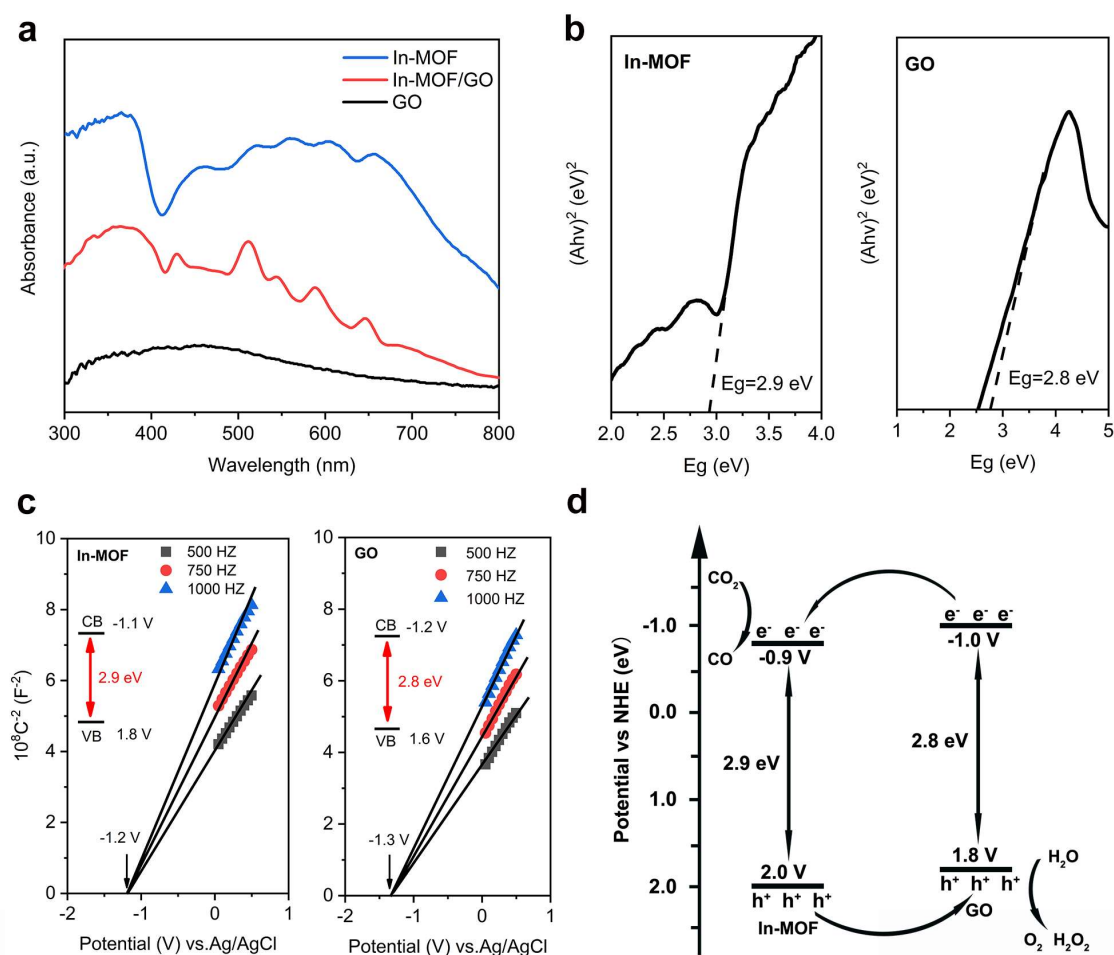
Response:

We thank the reviewer for the valuable suggestion. Based on this comment, we have added relevant tests, please refer to the figure below. UV-vis spectra were used to generate Tauc plots to determine the bandgap energies (**Supplementary Fig. 16a**). From the Tauc plots (**Supplementary Fig. 16b**), we determined that the bandgaps of In-MOF and GO are 2.9 eV and 2.8 eV, respectively. The Mott-Schottky plots (**Supplementary Fig. 16c**) show positive slopes for both In-MOF and GO, indicating that both materials are n-type semiconductors. The flat-band potentials of In-MOF and GO were found to be -1.2 V and -1.3 V vs. Ag/AgCl, respectively. Considering that the conduction band potentials of n-type semiconductors are typically 0.1 V more negative than the flat-band potentials, the conduction band potentials of In-MOF and GO are therefore -1.1 V and -1.2 V vs. Ag/AgCl, respectively. Taking the band gap into account, the band structure of In-MOF was determined with conduction and valence band potentials of -0.9 V and 2.0 V vs. NHE, respectively, while GO's conduction band and valence band potentials were found to be -1.0 V and 1.8 V vs. NHE, as shown in the band structure diagram in **Supplementary Fig. 16d**. Given the interlaced band structure between In-MOF and GO, and the fact that both are n-type semiconductors, it is likely that In-MOF and GO form a type-II heterojunction, with

electrons transfer occurring from GO to In-MOF and hole transfer from In-MOF to GO.

This is further supported by both XPS and theoretical analyses, which confirm that electrons transfer from GO to In-MOF at their interface. This transfer direction aligns with the experimentally calculated conduction band levels that GO has a more negative conduction band than In-MOF, further supporting the formation of type-II heterojunction between In-MOF and GO.

In this type-II configuration, the hybrid catalyst has a conduction band potential (-0.9 V of In-MOF) that is more negative than that required for CO₂ reduction to CO (-0.53 V), and a valence band potential (+1.8 V of GO) more positive than that require for 2e- and 4e- oxidation of water (+1.78 V and +1.23 V, respectively). Therefore, the In-MOF/GO heterojunction is theoretically capable of simultaneously facilitating both CO₂ reduction and water oxidation.



Supplementary Fig. 16. (a) UV-vis spectra of In-MOF, In-MOF/GO and GO; (b) Tauc plots of In-

MOF and GO; (c) Mott–Schottky plots of In-MOF and GO; (d) Schematic illustration of the band structure of In-MOF/GO.

Changes in Manuscript:

We have added the following discussion to the "**Investigation of preferential CO₂ adsorption**" section:

“The bandgaps of In-MOF and GO were determined using Tauc plots derived from UV-vis spectroscopy, while the conduction band potentials were established through Mott-Schottky analysis, allowing for the construction of the band structure diagram. In-MOF exhibits a less negative conduction band level (-0.9 V vs. NHE) compared to GO (-1.0 V), but a more positive valence band level (2.0 V vs. NHE) than GO (1.8 V). As a result, they are likely to form a type-II heterojunction, with the electron transfer occurring from GO to In-MOF and hole transfer from In-MOF to GO (Supplementary Fig. 16).”

Changes in Supporting Information:

Supplementary Fig. 16 has been added, along with the discussion:

“UV-vis spectra were converted into Tauc plots to determine the bandgap energy (Supplementary Fig. 16a). From these Tauc plots (Supplementary Fig. 16b), we determined that the bandgaps of In-MOF and GO are 2.9 eV and 2.8 eV, respectively. In the Mott-Schottky plots (Supplementary Fig. 16c), In-MOF and GO both exhibit positive slopes, indicating that both are n-type semiconductors. The flat-band potentials of In-MOF and GO were found to be -1.2 V and -1.3 V vs. Ag/AgCl, respectively. Considering that the conduction band potentials of n-type semiconductors are typically 0.1 V more negative than their flat-band potentials, the conduction band potentials of In-MOF and GO were determined to be -1.1 V and -1.2 V vs. Ag/AgCl, respectively. Based on the 2.9 eV bandgap of In-MOF, its valence band potential was calculated to be 1.8 V vs. Ag/AgCl; while for GO with a bandgap of 2.8 eV, the valence band potential was determined to be 1.6 V vs. Ag/AgCl. After converting between Ag/AgCl and NHE, the conduction and valence band potential of In-MOF is -0.9 V and 2.0 V vs. NHE, respective; for GO, its conduction and valence band potential is -1.0 V and 1.8 V vs. NHE, respectively. Therefore, we illustrated the band structure diagram as Supplementary Fig. 16d, which clearly shows that In-MOF and GO are likely to form a type-II heterojunction.”

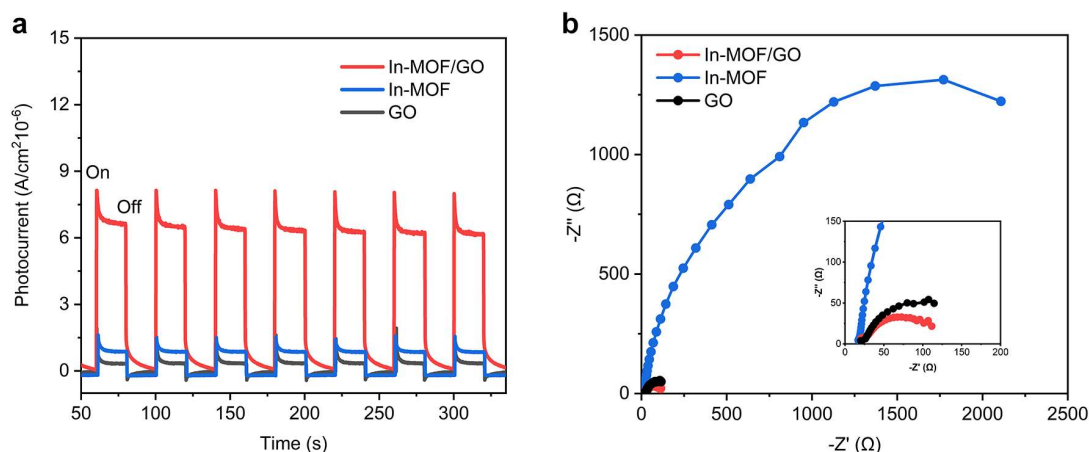
3. Comment:

What role does GO play during the photocatalytic reactions in this study?

Response:

We are very grateful to the reviewer for raising this question. In response to Comment 2, we have included a band structure diagram for the hybrid In-MOF/GO, which demonstrates that In-MOF and GO form a type-II heterojunction. This type-II configuration promotes charge separation between In-MOF and GO, as confirmed by photocurrent measurements and electrochemical impedance spectroscopy (EIS) analysis shown in **Supplementary Fig. 17**. In the photocurrent measurements, the photocurrent of In-MOF/GO is 7 and 10 times higher than that of individual In-MOF and GO, respectively. EIS analysis further shows that the hybrid structure exhibits significantly lower impedance, supporting the improved electron-hole separation efficiency in the hybrid catalyst, due to the formation of the type-II heterojunction.

In fact, few individual MOF catalysts can perform both kinetically challenging CO₂ reduction and water oxidation efficiently. Constructing a hybrid catalyst to enhance charge separation and independently conduct these half-reactions is often necessary. In this configuration, GO plays the role to form type-II heterojunction with In-MOF, and based on the direction of charge transfer, the water oxidation reaction is primarily expected to occur on the GO component.



Supplementary Fig. 17. Photocurrent measurements (a) and electrochemical impedance spectroscopy (b) for In-MOF/GO, In-MOF, and GO.

Changes in Manuscript:

We have added the following discussion to the " Investigation of preferential CO₂ adsorption" section:

“The formation of the heterojunction was further confirmed by photocurrent and electrochemical impedance spectroscopy (EIS) measurements, which indicate that the hybrid In-MOF/GO exhibits significantly enhanced electron-hole separation capabilities compared to individual In-MOF or GO (Supplementary Fig. 17)”

Changes in Supporting Information:

Supplementary Fig. 17 has been added, along with the discussion:

“In the photocurrent measurements, the photocurrent of In-MOF/GO is 7 and 10 times higher than that of individual In-MOF and GO, respectively. EIS analysis further shows that the hybrid structure exhibits significantly lower impedance, supporting the improved electron-hole separation efficiency in the hybrid catalyst, due to the formation of the type-II heterojunction.”

4. Comment:

It is recommended to provide more experimental details of photocatalytic tests, including the light intensity, the thickness and light transmittance of the PTFE film.

Response:

We thank the reviewer for the valuable suggestion. During the photocatalytic test, the intensity of the xenon lamp was maintained at $300 \text{ mW} \cdot \text{cm}^{-2}$. The PTFE membrane used had a thickness of $180 \mu\text{m}$, its transmittance was calculated as the ratio of transmitted light intensity through the PTFE membrane to the incident light intensity, which was found to be 20%.

Changes in Manuscript:

We have added information regarding the light intensity, the thickness and light transmittance of the PTFE film "Activity test of the photocatalytic CO₂ reduction" section. The descriptions are highlighted in yellow in the manuscript.

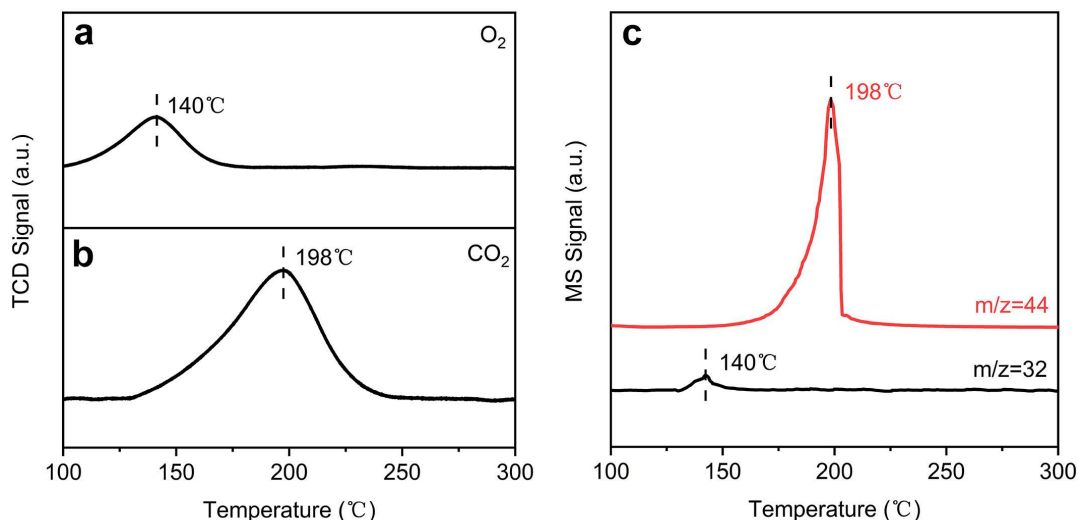
5. Comment:

To comprehensively investigate the chemisorption properties and interfacial interactions of the photocatalyst with carbon dioxide and oxygen, it is imperative to perform temperature-programmed desorption (TPD) experiments using pure CO₂, O₂, and a CO₂/O₂ mixture. This analytical technique will provide valuable insights into the adsorption capacity and the strength of the bonding between the catalyst surface and the adsorbate molecules.

Response:

We thank the reviewer for the valuable suggestion. In response, we conducted temperature-programmed desorption (TPD) experiments; please refer to the figure below. Under a pure O₂ atmosphere, a desorption peak appeared at around 140 °C (**Supplementary Fig. 21a**). By contrast, in a pure CO₂ atmosphere, the desorption peak shifted to a higher temperature of 198 °C (**Supplementary Fig. 21b**). The higher desorption temperature indicates that more energy is required for the desorption of CO₂ molecules from the In-MOF/GO surface, suggesting a stronger interaction between CO₂ and the surface active sites of In-MOF/GO compared to O₂. Additionally, the TPD analysis under pure CO₂ atmosphere showed a larger peak area, indicating that In-MOF/GO has a higher adsorption capacity for CO₂ than for O₂. This result suggests that In-MOF/GO has a stronger affinity and higher adsorption capacity for CO₂.

Furthermore, to investigate behavior in a CO₂/O₂ mixture, we performed a TPD-MS analysis under a 1:1 (v/v) CO₂ and O₂ mixed atmosphere (**Supplementary Fig. 21c**). The desorption of CO₂ (mass peak $m/z=44$) occur at 198 °C with a notably larger peak area, while O₂ desorbed ($m/z=32$) at 140°C, consistent with the results using pure gases. This analysis further confirms that In-MOF/GO has a strong adsorption capability and selectivity for CO₂, allowing it to preferentially adsorb CO₂ even in a mixed gas environment. This selectivity advantage position In-MOF/GO as an effective catalytic material for CO₂ capture and conversion processes.



Supplementary Fig. 21. Temperature-programmed desorption (TPD) analysis of In-MOF/GO under pure O₂ (a), pure CO₂ (b), and 1:1 (v/v) CO₂/O₂ mixture (c).

Changes in Manuscript:

We have added the following discussion to the "**Investigation of preferential CO₂ adsorption**" section:

*“Furthermore, we conducted temperature-programmed desorption (TPD) experiments to verify the preferential adsorption capability of CO₂ (**Supplementary Fig. 21**). The results showed that CO₂ exhibited a larger desorption peak area and a higher desorption temperature compared to O₂, indicating that In-MOF/GO possesses strong selectivity and stability for CO₂ adsorption, allowing it to preferentially adsorb CO₂ even in the presence of competing gases such as O₂.”*

Changes in Supporting Information:

We have added Supplementary Fig. 21 to Supporting Information, along with the discussion:

*“Under a pure O₂ atmosphere, a desorption peak appeared at around 140 °C (**Supplementary Fig. 21a**). By contrast, in a pure CO₂ atmosphere, the desorption peak shifted to a higher temperature of 198 °C (**Supplementary Fig. 21b**). The higher desorption temperature indicates that more energy is required for the desorption of CO₂ molecules from the In-MOF/GO surface, suggesting a stronger interaction between CO₂ and the surface active sites of In-MOF/GO compared to O₂. Additionally, the TPD analysis under pure CO₂ atmosphere showed a larger peak area, indicating that In-MOF/GO has a higher adsorption capacity for CO₂ than for O₂. This result suggests that In-MOF/GO has a stronger affinity and higher adsorption capacity for CO₂.*

*Furthermore, to investigate behavior in a CO₂/O₂ mixture, we performed a TPD-MS analysis under a 1:1 (v/v) CO₂ and O₂ mixed atmosphere (**Supplementary Fig. 21c**). The desorption of CO₂ (mass peak $m/z=44$) occur at 198 °C with a notably larger peak area, while O₂ desorbed ($m/z=32$) at 140°C, consistent with the results using pure gases. This analysis further confirms that In-MOF/GO has a strong adsorption capability and selectivity for CO₂, allowing it to preferentially adsorb CO₂ even in a mixed gas environment.”*

6. Comment:

As mentioned in this manuscript: “electron densities on the GO and In-MOF moieties decrease and increase, respectively, indicating electron transfer from GO to In-MOF during the formation of the heterostructure” . What is causing this phenomenon, and what is the underlying driving force?

Response:

We are very grateful to the reviewer for raising this question. We believe that there are two primary reasons for the potential driving force that leads to electron transfer from GO to In-MOF. First, based on the calculation results, there is a difference in electronegativity: the metal nodes of In in In-MOF typically have a higher electronegativity, which attracts electrons. In contrast, although GO contains abundant oxygen-containing functional groups, its overall electronegativity is relatively lower. This difference in electronegativity causes electrons to transfer from the less electronegative GO to the more electronegative In-MOF. Additionally, the electron transfer is also influenced by the difference in energy levels between the two materials. As shown in the band diagram (Response to Comment 2), the conduction band potential of GO is higher than that of In-MOF, leading to a tendency for electrons to flow from GO to In-MOF to achieve energy level alignment. This difference in energy levels promotes the transfer of electrons from GO to In-MOF, thereby facilitating charge separation.

We have made every effort to improve the manuscript and have made some changes to the manuscript. These changes do not affect the content or framework of the paper. In this revised version, changes to our manuscript are highlighted in yellow in the document.

We sincerely thank the editors/reviewers for their enthusiastic work and hope that these changes will be acknowledged.

Once again, thank you very much for your comments and suggestions.